NJC

New Journal of Chemistry

A journal for new directions in chemistry

Accepted Manuscript

NJC

New Journal of Chemistry

A journal for new directions in chemistry

rsc.li/njc

Volume 42
Number 6
21 March 2018
Pages 3963-4776

ISSN 1144-2546

PAPER
Chechia Hu, Tzu-Jen Lin et al
Yellowish and blue luminescent graphene oxide quantum dots prepared via a microwave-assisted hydrothermal route using H2O2 and KMnO4 as oxidizing agents

ROYAL SOCIETY OF CHEMISTRY

Cnrs

ROYAL SOCIETY OF CHEMISTRY

rsc.li/njc

Copper (II) ions Supported on Functionalized Graphene Oxide: An Organometallic Nanocatalyst for Oxidative Amination of Azoles via C–H/ C-N Bond Activation

Masoumeh Behzadi,*[a] Mohammad Mahmoodi Hashemi,*[a] Mostafa Roknizadeh,[a] Shahrokh Nasiri,[a] Ahmad Ramazani Saadatabadi[b]

Graphene oxide (GO) was chemically modified with *para-aminobenzoic* acid (PABA) to immobilize copper (II) ions to its surface and used as a nanocatalyst for the oxidative C (sp²)–H bond amination reaction. A practical method to prepare Cu^{+2} supported on *para-aminobenzoic* acid grafted on GO was reported. Prepared Cu^{+2}@GO/PABA was characterized by FT-IR, XRD, SEM, AFM, TEM, UV-Vis, and ICP techniques. The results showed that the morphology, distribution, and loading of copper ions could be well-adjusted by grafting of PABA on GO. Moreover, just 2 mol % of Cu^{+2}@GO-PABA could catalyze the C–H activation reaction of benzoxazole and benzothiazole with secondary amines in >94% yields. Also, the catalyst showed very good recyclability and very less leaching of the Cu to the reaction solution. The high activity of Cu^{+2}@GO-PABA can be ascribed to the good synergistic effects of Cu^{+2} and *para-aminobenzoic* acid grafted on graphene oxide.

1. Introduction

The transition-metal-catalyzed selective C-N bond formation reaction of azoles is an efficient approach in synthetic organic chemistry, whereas five-membered heterocyclic compounds with amine groups are widely applicable in biological, pharmaceutical, and material sciences.[1] Many synthetic methods, including cyclo condensation reactions from two functionalized precursors (e.g. Hantzsch aminothiazole synthesis),[2] palladium-catalyzed Buchwald-Hartwig coupling[3] and copper-catalyzed Ullmann and Goldberg coupling, have been developed to access this vital motif.

With great advancement in the C-H activation reaction, it seems some difficulties, such as high-temperature, long reaction-time, toxic functionalization, and use of a large amount of expensive metal oxidant and strong acid or base, have not been provided yet.

A pioneer and engaged two-dimensional (2D) carbon nanostructure, graphene oxide (GO), has fascinated exclusive attention in catalysis, photochemistry, electrochemistry, and organic catalysis, during the past decays. [4-8] The substances based on graphene material keep incomparable structural features and generating extraordinary physical properties, such as high surface area, high water dispersal status, innate low mass, easy surface adjustments, and plenty of oxygen-carrying functionalities, [9-11] which are promising application as catalysts or supports.

Graphene, a single layer of carbon atoms arranged in a honeycomb lattice, regarded as an efficient applicant for abundant state-of-the-art technologies, such as nanoelectronics,[12] transparent conducting electrodes,[13] composites,[14] supercapacitors,[15] gas sensors,[16] and hydrogen storage [17] because of its fascinating electronic, mechanical, thermal properties, and large specific surface areas.[18-26] Between the chemical approaches of GO generation, rough oxidation of the graphite is the most compatible and easily large-scale procedure to prepare GO.[27] Due to the abundant oxygen containing functional groups on its basal sheet (phenol, hydroxyl, and epoxide groups) and at its edges (carboxylic groups), Conspicuously, GO displays a remarkable hydrophilic inherent and significantly distributable in water and many organic solvents.[28] As a result, the defects and multiple functional groups, authorize GO to be a preferential candidate for further chemical functionalization with different materials such as, surfactants, polymer, alkaloid, organometallic compounds, and metal nanoparticles. [29-32] which are greatly applicable as catalysts or supports. In addition, setting down the organometallic compounds, nanoparticles or metal ions on functionalized graphene oxide makes also a significant state for recovery and recyclability of the catalysts, forming cross-linked structures, with substantially improved mechanical and electronically properties.

In this study, we investigated a C-H activation, C-N bond formation of benzoxazole and benzothiazoles with secondary amines and O_2 as a green oxidant. However, the success of this synthetic procedure relies on employing a recoverable organometallic nanocatalyst which is used in a few amounts. To achieve this goal, we surveyed if the exploiting of chemical optimized-graphene oxide with primary amine to immobilize copper (II) ions to accomplishing a better function of catalytic for C (sp²) –H bond amination reaction. So, a facile and novel method to prepare copper salt of para-aminobenzoic acid (PABA) grafted on graphene oxide materials (Cu^{+2}@GO-PABA) was firstly reported which could catalyze C-H/ C-N reaction of benzoxazole and benzothiazoles with various secondary amines with good yields.

2. Experimental section

2.1 General Information

The extra pure graphite powder, $CuCl_2 \cdot 2H_2O$, $KMnO_4$, H_3PO_4, H_2SO_4 (96-98%) and HCl (37%), H_2O_2 (30%), benzoxazole, para aminobenzoic acid, sodium carbonate, various amiones, and all of solvents and other marerials were purchased from Sigma-Aldrich and Merck companies. Ultrapure deionized water (resistivity >18

a. Department chemistry, Sharif university of Technology, Tehran, Iran. Email: masome.behzadi@gmail.com

b. Department of Chemical and Petroleum Engineering, Sharif university of Technology, Tehran, Iran

MΩ) was obtained from a Mili-Q Biocel system. The morphology and size of Cu@GO-PABA were studied by Scanning Electron Microscopy (SEM; TESCAN–MIRA 3) and Transmission electron microscopy (TEM, CM30 300kV). The XRD patterns of Cu-GO/PABA nanohybride were determined via INEL EQUINOX 3000 X-ray diffractometer, using Cu Kα radiation, to determine structural changes and d-spacing. EDAX analysis was performed using MIRAPLMU for elemental analysis. A Raman spectrometer (Takram p50C0R10) equipped with a laser with a working frequency of 532 nm as its excitation source was used to approve the Cu@GO/PABA compared to GO and GO-PABA structures. UV visible spectra were obtained using a Unico 4802 spectrophotometer. IR spectra were recorded on Bruker Tensor-27 FTIR spectrometer using KBr pellets. The amount of copper in catalysts was identified by inductively coupled plasma atomic emission spectroscopy (ICPAES WFX-120). All of the known C-H amination of benzoxazole compounds were identified by comparison of their spectral data and physical properties with those of the authentic samples. Other new products were characterized with 1HNMR and 13CNMR spectra (Bruker DRX-300 AVANCE NMR spectrometer) using CDCl3 as a solvent and using tetramethylsilane (TMS) as an internal standard. Chemical shifts were reported in parts per million (δ) downfield from TMS. All coupling constants (J) are in hertz. Also, Mass spectrometer operating at an ionization potential of 70 ev.

2.2 Synthesis of GO

Graphene oxide (GO) was synthesized from the oxidation of extra pure graphite powder by the modified Hummer's method.[33] Briefly, 1.0 g graphite powder was mixed to 120 mL concentrated H_2SO_4 and 13 mL H_3PO_4 85% was stirred in a room temperature for 1 h. Then 6.0 g $KMnO_4$ were added stepwise to this solution during the 30 minutes with stirring at 50°C. Then the reaction maintained about 50°C and stirred for 12h. After this time, 200-250 mL distilled water slowly was added to the green suspension with stirring while the reaction temperature kept in 0°C. Next, 2-3 mL H_2O_2 30% was added slowly to reduce the excess $KMnO_4$ whereas color of solution rapidly changed from green to yellow. The prepared graphene oxide could be easily centrifuged at 5,000 rpm and washed with HCl solution (30 mL, 1 M) and DI water 3 times successively. Finally, the crude brown product was dried in vacuum oven 24h at 40°C. The weight of dried GO was 2.30 g.

2.3 Synthesis of Graphene Oxide para-Amino Benzoic Acid (GO-PABA)

Prepared GO (2.30 g) dispersed in ethyl acetate (30 ml) by sonication bath for 5 minutes. Then para-aminobenzoic acid (1.75 g, 7.5 mmol) was added to exfoliated GO. The reaction mixture was then refluxed while being stirred magnetically at 80 °C for 16 h. The mixture was cooled to room temperature and filtered. The solid mass was washed with ethyl acetate by a soxhlet for 10 h in order to remove all unreacted para-aminobenzoic acid. The solid was dried in an oven at 100 °C to gain 3.56 g black solid product.

2.4 Grafting of Cupper ion nanoparticle on Amine functionalized Graphene Oxide (Cu+2@GO-PABA nanocatalyst)

This process has 2 steps. All of procedure summarized in scheme 1. Firstly, sodium salt of the para-aminobenzoic acid (GO-PABA-Na+) was prepared via dispersing of 1.15 gr GO/PABA in 30 ml of DI water for 30 minute in ultra-sonication bath then a saturated solution of sodium carbonate (4.11 gr, 30 ml DI water) was added to

give the black sodium salt. This result dried and soxhelet with DI water to remove of sodium adsorbed on the GO/PABA surface. Finally, 2.5 gr black powder product was obtained. Furthermore, for preparation of Cu-GO-PABA nanocatalyst, sodium salt of GO/PABA (0.3 gr) was dispersed in 10 ml DI water in 10 minutes in a round-bottomed flask to obtain the homogenous suspension and then treated with 10 ml solution of $CuCl_2$ (10 wt %) and refluxed at 100°C for 2h. Subsequently, the solution stirred at ambient temperature for 24 hr. after completion of the reaction, the crude product filtered and dried in room temprature. The obtained gray-black solid was washed with deionized water for 10 hrs (soxhelet) and dried in an oven at 40°C for 5 hours to give 0.63 gr copper nanocatalyst.

2.5 General procedure for copper-catalyzed oxidative C-H activation-direct amination of benzoxazoles and benzothiazole with secondary amines

In a round bottom flask equipped with a stirring magnetic bar and a condenser, azoles (0.5 mmol) 1, amine (0.6 mmol) 2a-i, nanocatalyst Cu+2-GO-PABA (2 mol %), CH3COOH (120 μl), and CH3CN (2 mL) were mixed. Then the pure O2 injected to the reaction mixture. The suspension was stirred and refluxed at 70 °C for 12 h. After completion of the reaction, the mixture was cooled to room temperature, filtered from nanocatalyst and washed with 10 ml chloroform to extract the pure products with (32-94%) yield.

3. Results and discussion

The designed synthetic process for functionalized-GO/metal nanocomposite is shown in Scheme 1. This strategy for the synthesis of the activated nanocatalyst relies on three simple steps. First, the exfoliated graphene oxide (GO) nanosheets were prepared from natural graphite by the modified Hummer's method.[33] Furthermore, to eliminate the generated toxic gases, a mixture of H2SO4/H3PO4 (9:1 volume ratio) was used instead of H2SO4 as a novel approach.[41] In this method graphene oxide (GO) nanosheets have usually a size between tens to several hundreds of square nanometers.

Second, In the process of fabricating the new activated GO-Cu nanocatalyst, we used para-aminobenzoic acid (PABA) to adjust functionalization of graphene oxide and immobilization of Cu+2 on the surface of the functionalized GO-PABA is chemically grafted on surface GO and increase the carboxyl functional group for covalently chelating Cu on the GO surfaces.

The third key process for preparing GO nanocomposite, the para-aminobenzoic acid supported on GO is reacted with $CuCl_2$ to give its copper salts as a GO-PABA/Cu+2 which is new and efficient nanocatalyst.

As shown in Scheme 1, the oxygen-containing groups on GO, such as carboxyl and hydroxyl groups, were removed under thermal treatment as a reducing agent. The color of the solution changed from brown-yellow to dark brown, indicating the removal of some oxygen functional group. To increase the loading Cu on the GO, and preventing of releasing various oxygen functional groups, we improved the activity of GO substrate with PABA that keep the especially carboxylic acid group on the GO surface, as a result of chemical bonds formed between functional groups of GOs and Cu

ions. Also, metal leaching is decreased due to this chemical reaction.
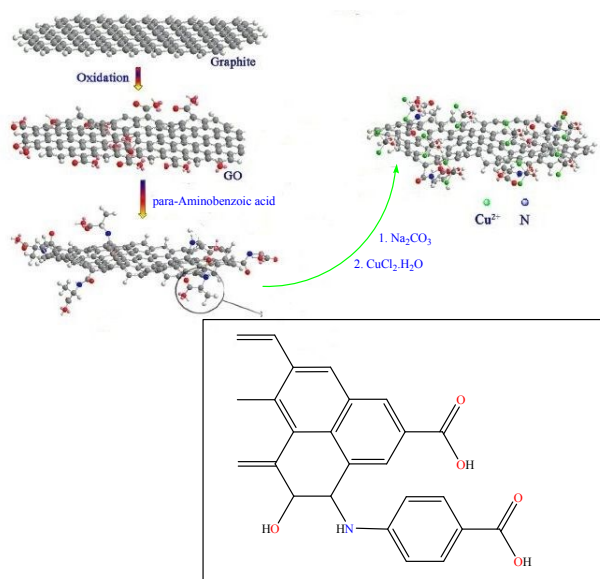
Scheme 1. Synthesis steps of Cu@GO-PABA nanocatalyst.

Morphological, compositional, and structural characterization of the nanocomposite were analyzed with a number of methods including scanning electron microscopic (SEM), transmission electron microscopic (TEM), XRD, EDX, Raman spectroscopy, Uv-visible and FT-IR analyse. To investigate the chemical structure changes of GO after functionalization, the FTIR spectrum of the nanocomposite powders in each processing step for GO, GO-PABA, and GO-PABA-Cu^{+2} were taken which were shown in Figure 1. Considerable changes can be observed among the FT-IR spectra of GO and GO-PABA. GO has some characteristic peaks, O-H stretching vibration peak was observed at 3371, while carboxyl/carbonyl groups had stretching peak at 1732, C=C aromatic bands displayed at 1627, C-O related epoxide/ether group was at 1285, and C-O at alkoxy functional group was conceived at 1174 cm^{-1}. After grafting PABA on the GO, the carboxyl (C=O, 1732) and O–H stretching vibration peaks (3371) of GO were disappeared while epoxy and alkoxy bands at 1285 and 1122 cm^{-1} appeared and intensified.

Upon treatment with PABA, two new bands at 1561, and 1516 cm^{-1} appeared in the spectrum, which can be assigned to the coupling of the C-N stretching vibration with N-H deformation vibration while broadband peak at 3012 cm^{-1} is contributed to the N-H stretching vibration that is overlapped with O–H stretching vibration in carboxylic acid functional group on PABA and other hydroxyl groups in GO support, also, strong peak at 1698 cm^{-1} is attributed to C=O stretching in carboxylic group on PABA. So, the broad peaks at 3012 and strong peak 1698 cm^{-1} are attributed to the characteristic carboxylic group on the para-aminobenzoic acid. Furthermore, the presence of peaks at 2890 cm^{-1} was associated with the stretching vibrations of C-H aliphatic on GO/PABA. These results indicate the successful attachment of PABA units on the GO nanosheet surface.

When GO chemically reacted and bonded to Cu salts, its characteristic peaks were vanished. For example, the C=O, OH, and epoxide vibration stretching peaks disappeared whereas the intensity of alkoxy (C-O) band increased. Reducing carbonyl bond in

carboxylic functional group in 1703 cm^{-1} approved the coordination between carboxylic acid and a Cu^{2+} ion. In addition, by treatment with Cu^{2+}, the epoxide group participates in the ring-opening reaction, then the its relative intensity of stretching vibration decreased, as a result, the intensity of alkoxy stretch enhanced.[35]

On the other hand, vanishing OH broad peak at about 3371 cm^{-1} is related to interaction between copper (II) ions with OH functional groups, and peaks in 3447 and 3337 cm^{-1} are contributed to the N-H stretching vibration. These results support that chemical interactions between GO and Cu^{+2} occurred and due to bearing the plenty of active oxygenating functional groups (epoxide, hydroxyl, alkoxy, and carboxylic acid), both the basal plane and edges of GO, completely attached to Cu salts. Consequently, Cu nanoparticles are nucleated in whole of GO surface and edges.
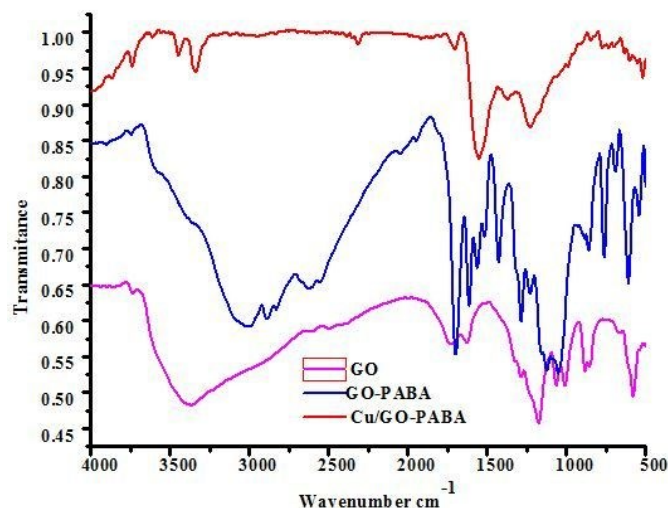
Figure 1. FT-IR spectra of (a) GO, (b) GO-PABA and (c) Cu@GO-PABA

The pristine GO distinguished through two fingerprint peaks in Uv-vis, 251 nm and 300 nm (shoulder peak), related to the C=C and C=O transmission. As demonstrated conspicuously in Figure 2., one of GO discriminative peaks that attributed to C=O and other oxygen functional groups, has been improved in GO-PABA and also the absorption is red-shifted with a maximum at 269 nm. The visible wavelength absorption and dark color of GO solution imply the regeneration of the conjugated C=C lattice clearly.[36]
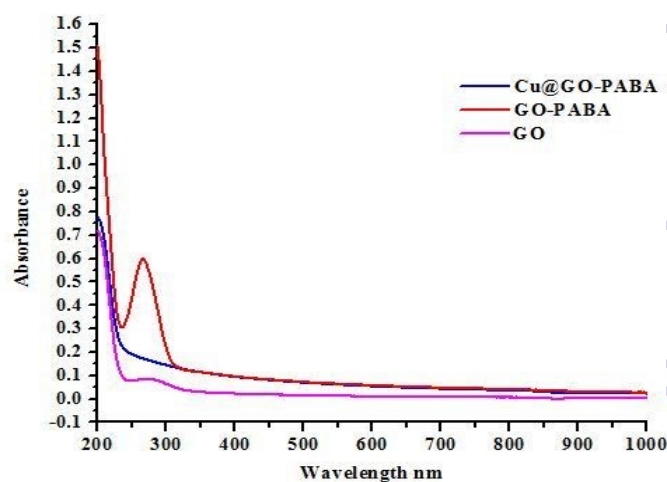
Figure 2. Photographs and UV-vis spectra of 0.mg/mL solution of GO, GO-PABA, and Cu@ GO-PABA in water.

The functional groups bearing heteroatoms (oxygen, nitrogen) on GO and GO-PABA surfaces have a significant role in the immobilization of metal ions. It is obvious that the negative charges on the GO substrate develops a nucleus for the growth of positive metal ions on the GO and GO-PABA. UV-vis demonstrates that Cu ions can be easily grafted on the GO-PABA surface. The characteristic dark color of Cu materials in solution with no distinct absorption band at 300–1000 nm is also evident in Cu^{+2}@GO-PABA. Raman spectroscopy of the nanocomposite powders indicates changes of oxidation states in the GO during processing functionalization and coating with the metal process (Figure 3). In the Raman spectrum, GO has two characteristic peaks, G-band and D-band. The G-band comes from the E_2g symmetry related to sp^2 carbons (graphite network), and the disorder ones, D-band generated through the chemical defects that the oxygenated functional groups on basal and edges surface create on graphene lattice.[37]

As shown in Figure 3, the peaks in GO (1350 $cm^{–1}$), GO-PABA (1355), and Cu@GO-PABA (1350 $cm^{–1}$) are characterized as a D-band. In addition, the peaks at 1602 cm^{-1} in all panels, related to G-band that makes by the the E_2g symmetry of the sp^2 C atoms.

Furthermore, the ratio of the D band to the G band is a measure of defects present in the GO, GO-PABA, and Cu@GO-PABA. This amount is 0.877 for GO, 0.875 in GO-PABA and 0.89 after grafting Cu on GO/PABA surface. A higher value may indicate higher defect density. Based on figure 3, in GO and GO/PABA peaks this value is relatively fixed that indicates after grafting para-aminobenzoic acid to GO substrate, any more defection has not been observed at graphene domains.

The I_D /I_G ratio increased from 0.87 (GO and GO/PABA) to 0.89 for Cu@GO/PABA because of the covalent chemical banding between GO-PABA and Cu ions that are resulted from the further defect and damage in the graphene sp^2 bonding lattice. As shown in figure 3, the oxidation process makes a continuous and adaptable coating of Cu^{+2} on the GO-PABA flakes that heighten the I_D /I_G ratios of the GO-PABA/Cu nanocomposite powders markedly due to the functionalization GO with PABA and grafting with Cu^{+2} process enhanced the functional groups and partially recovered the graphene oxide structure. Remaining defects in the GO serve as chemical bonding sites between the GO-PABA and Cu (II) ions. Also, in panel c, Raman bands at 97, 211 $cm^{–1}$ proves the stable formation of continuous Cu ions on GO.[38]
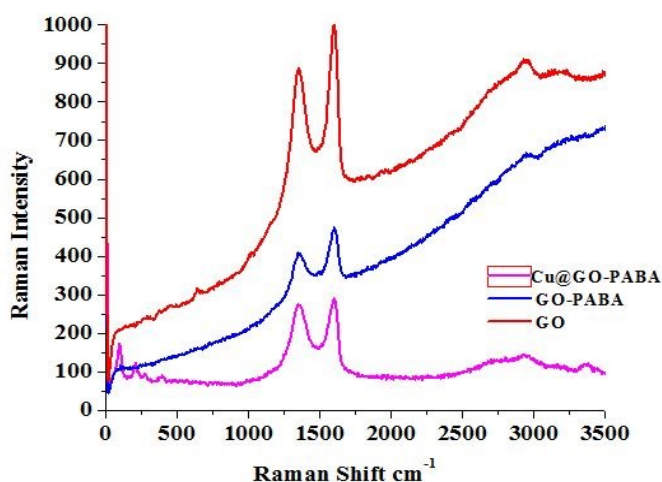

Figure 3. Raman spectra of GO (a), GO-PABA (b), and Cu@GO/PABA

The morphology and structural features of the GO and Cu@PABA-GO composites were examined highly by some spectroscopic analysis such as, XRD, scanning electron microscopy (SEM), and transmission electron microscopy (TEM). Figure 4 shows the XRD patterns of the as-prepared Cu@GO/PABA nanocomposites. The diffraction peaks at around 2θ= 16.1° and 17.5˚ correspond to the (001) GO XRD pattern. The interlayer of GO (0.54 nm) was calculated by the Scherer equation, which was much more larger than fresh graphite that is about 0.34 nm. Indeed, increasing the interlayer space in GO material resulted from to the presenting of oxygen-containing functional groups on the graphene sheet .[39]

The peaks at 32.2° (220), 32.5 (220), 39.6˚ (200) and 36.5˚ (111) were fixed with CuO and Cu_2O forms, respectively, and the coalescence of two crystal structures was identified at 48.2° (200) in Figure S6 of the Supporting Information.[40] All the peaks in the spectra can be assigned to orthorhombic CuO and Cu_2O (a = 6.8920 Å, b = 9.0800 Å, c= 6.0550 Å, α= 90.0000˚, β = 90.000°, γ= 90.000˚). None of obvious typical peaks belonging to rGO are observed in the XRD spectra of Cu@GO/PABA nanocomposites. It can attributed in slight amount and little diffraction intensity of rGO. In addition, the spectrum displays more negligible peak intensity than the CuO for the Cu_2O species, which suggest the CuO in the Cu@GO/PABA nanocomposites, comparatively has high crystalline structure, bearing high amount of oxygen functional groups (carboxylic, hydroxyl, and epoxy), intensifying the diffusion and crystallization of CuO grains on the GO surface.[40]
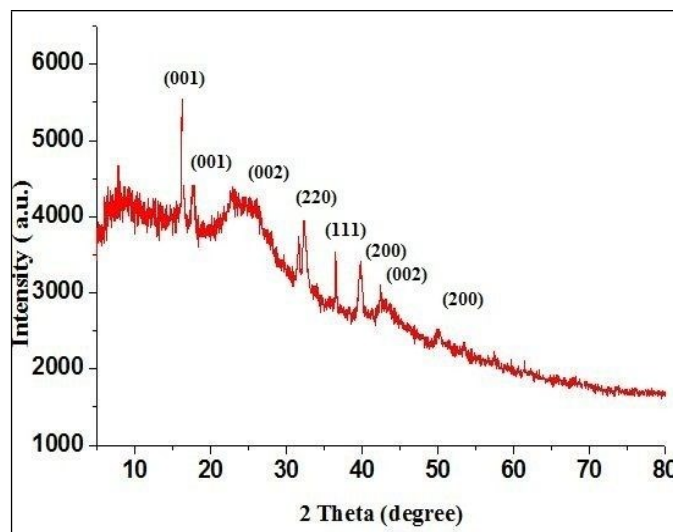

Figure 4. XRD image of Cu@GO-PABA

Figure 5 shows SEM images and EDX surface elemental analysis of copper catalyst nanostructures.

As can be shown, the 2D composite nanosheets with wrinkled and folded features could be observed in the PABA–GO-Cu material. However, the chemical interaction between amino groups at the edge and basal plane of GO and copper ions, enhances the stacking of PABA–GO-Cu hybrids more than that of GO.

Most of the Cu^{+2}@GO-PABA nanocatalyst are uniformly distributed on the GO sheet and keep away from the aggregation, which will greatly improve their catalytic properties. The GO-Cu (II)-PABA (Figures 5a) exhibits a rough bulky surface, probably due to the complexation with Cu (II) and coordination with the ligands. It can

be observed from the SEM images (Figure 5a) that the Cu^{+2}@GO/PABA are nearly spherical with an average size of 6-15 nm, respectively.

The EDX surface elemental analyses (Figures 5b and S5) further proved the presences of Cu and N atoms, indicating that the GO is bounded to copper, which in turn is coordinated to the energetic ligands.

Furthermore, according to the results of XRD characterization, the morphology of Cu materials on the GO-PABA support, were also recognized by TEM (as described in Figure 6). Thus, the immobilization of Cu NPs on the PABA-GO-Cu^{+2} surface principally were spherical (all patterns in Figure 6).

The Cu NPs on the surface of the PABA-GO-Cu^{+2} catalyst were mainly spherical (all panels Figure 6). However, a homogeneous dispersion of Cu ions was observed for our nanocatalyts at edge and base of GO surface (panel a, b). TEM showed the presence of 8.8-10.5 nm size Cu ions in large numbers on the aminated graphene oxide surface. Based on the panel c and d, a few Cu nanostructure like worm pattern can be seen, which implies that para-aminobenzoic acid reacted to graphene oxide has plentiful active sites including N and a π-conjugated system, and the multiple connection sites that result in massive aggregation of Cu nanomaterials. Also, GO has more oxygenated functional groups and the aggregation of Cu nanocatalyst was inevitable on these materials with rich O, N sites or a π-conjugated system. Also, to elucidate the quantitative correlation between O, N active groups and copper species, copper loading in the graphene oxide-based composites, was determined from the inductively coupled plasma analysis (ICP). However, loading of copper in these materials was about 14.5 wt %. The high amount of copper for PABA-GO-Cu nano catalyst may be attributed to rich amine group, oxygen active sites or aromatic rings, which could be created the main driving force for the affinity for Cu^{2+} ions.

In order to preparation of amino-benzoxazole and amino benzothiazole compounds and evaluate the catalytic activity of the PABA–GO–Cu nano composite in organic synthesis, direct oxidative C-H amination of benzoxazoles and benzothiazoles with secondary amines as a nitrogen source was investigated in Scheme 2.

X= O, S

1   **2**   **3, 4**
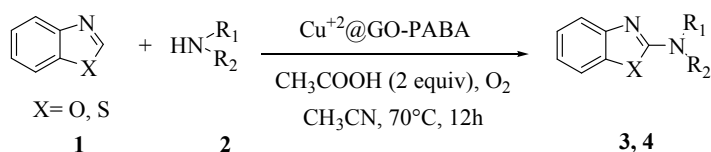
Scheme 2. Oxidative amination of azoles with secondary amine

To obtain the optimize reaction conditions, a set of experiments, as a benchmark reaction, were performed using benzoxazole (0.5 mmol) 1 and pypiridine (0.6 mmol) 2a for synthesis of corresponding N, N-2-amine benzoxazole 3a (Scheme 3).

1   **2a**   **3a**
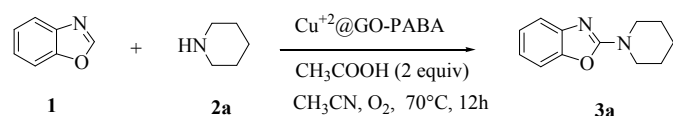
Scheme 3. Model reaction for optimization of reaction condition

Moreover, to optimize the amount of the catalyst, we performed a series of reactions with varying amounts of Cu^{+2}@GO/PABA (0.5-10 mol %). The data is given in Table 1. Astonishingly, the catalyst was found to be efficient (18-84 % yield) even in its minimum quantity (0.5 mol %). Hence, this amount of the catalyst was considered as its minimum quantity for a successful copper catalyzed C-H activation reaction with excellent yield and high purity. As shown in Table 1, the highest yield was obtained when 2 mol% of copper nanocomposite was used which was the optimize amount for our catalyst (entry 3). An increase in the amount of catalyst did not improve the yield of the reactions (entry 4-6).

Notably, in the controlled experiments of the reaction conditions, the optimal system for the coupling reactions was obtained using CH_3COOH (2 equiv) as an additive, CH_3CN as solvent at 70 °C and 1 atmosphere O_2.[34] The copper and the oxidizing reagent, O_2 have substantial role in the reaction procedure, so that in the lack of copper source and oxidant, the expected product yields reduced from 84% to 18 or 0%, respectively (Table 1, entry 7, 8).

Table 1. Optimization of Reaction Conditions of Benzoxazole and Pipyridine (Model reaction)

Entry	Cat. (mol %)	Oxidant (1atm)	Conversion (%)	Yield (%)
1	0.5	O_2	60	31
2	1	O_2	90	52
3	2	O_2	100	84
4	3	O_2	95	73
5	5	O_2	95	70
6	10	O_2	80	70
7	Opt amount	-	trace	18
8	-	O_2	N.R	N.R

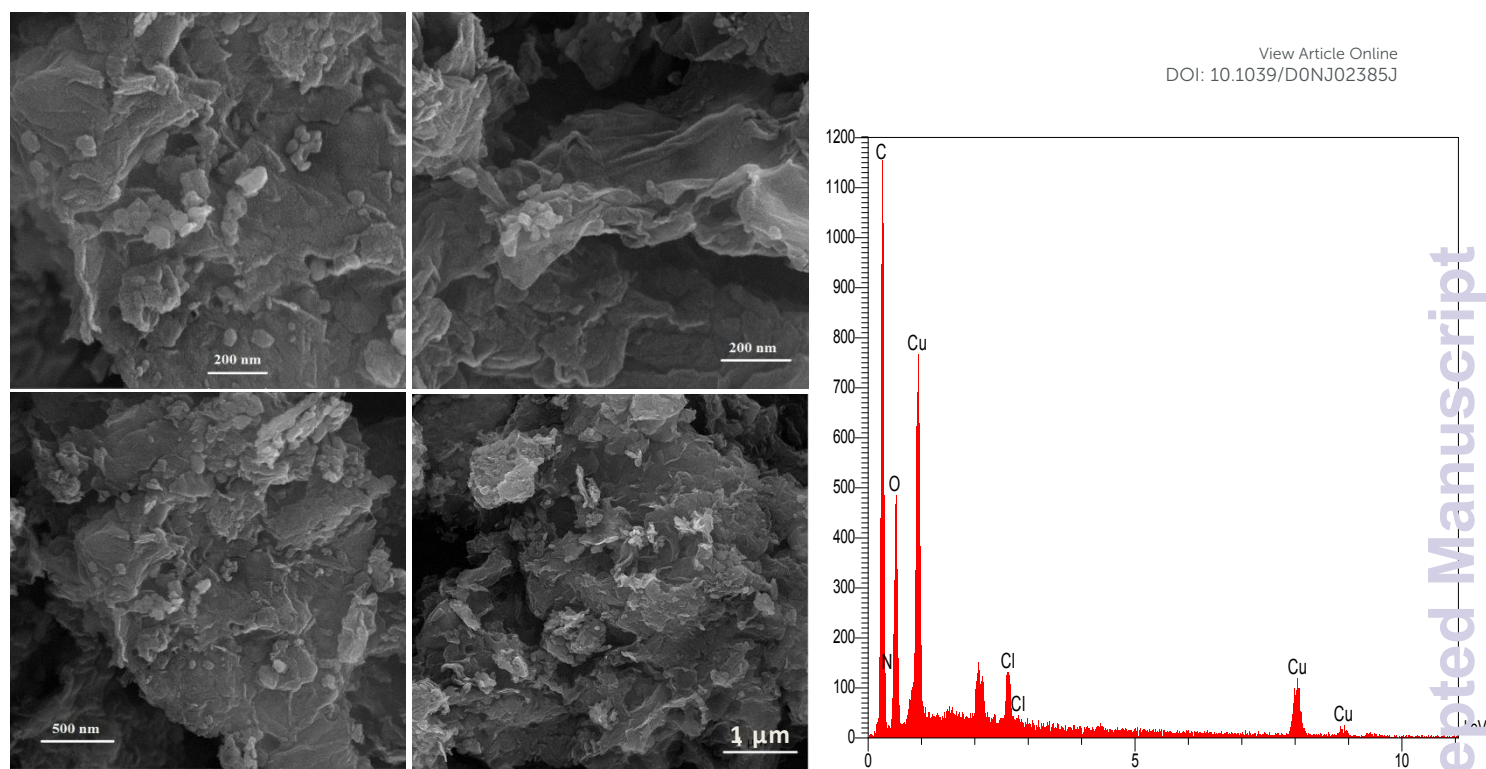Reaction conditions: Benzoxazole (0.5 mmol), pipiridine (0.6 mmol), CH_3CO_2H (2 eq), 70˚C, 12 h.

Figure 5. (a) SEM images of the Cu@GO-PABA catalysts, at 200 nm-1 µm size magnification (b) EDX images of the Cu@GO-PABA
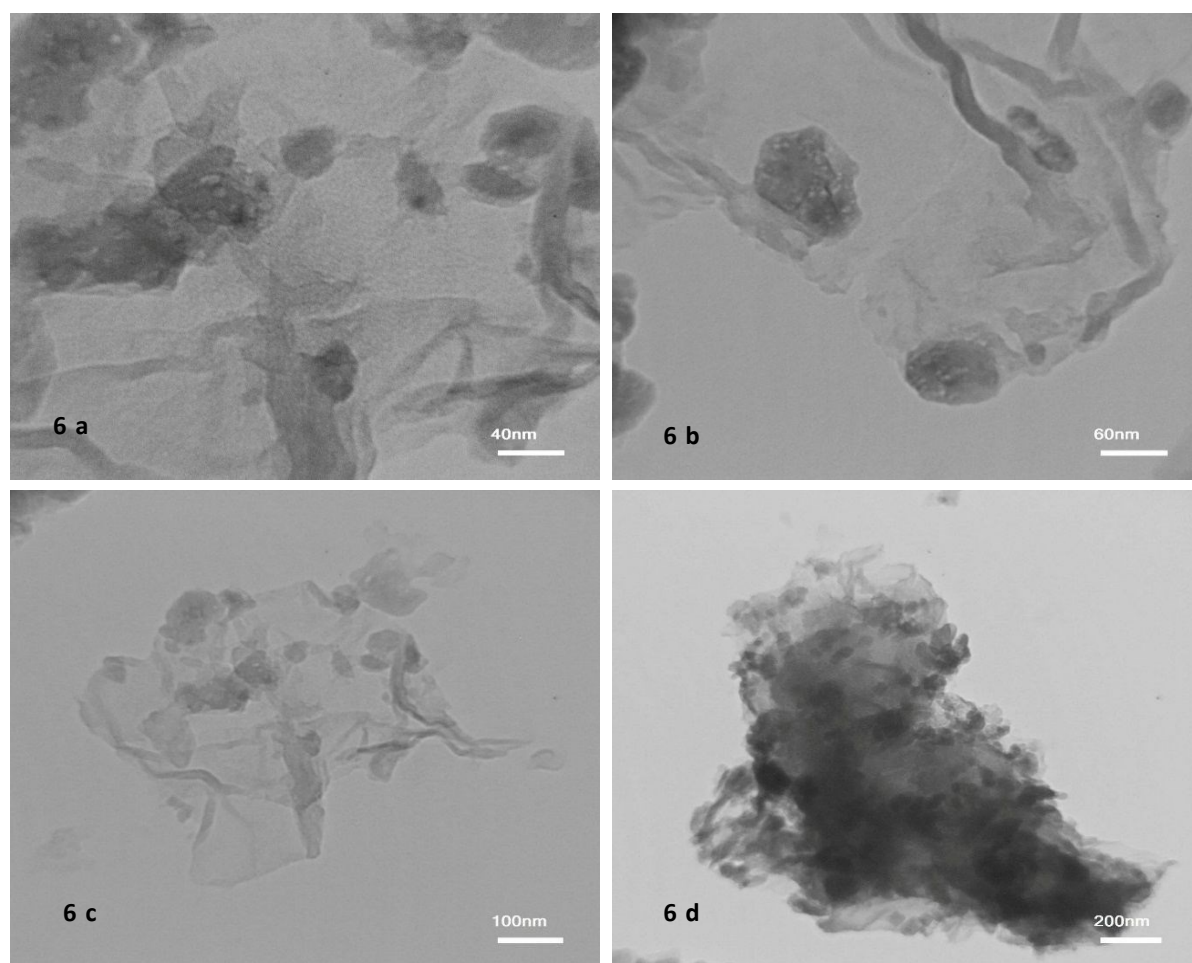

Figure 6. TEM images of PABA-GO-Cu

With best conditions in hand, direct amination of benzoxazole and benzothiazole was carried out with various amines (Table 2). The runs of this reaction were performed with aliphatic and cycloaliphatic amines including diethylamine, dipropylamine, diisopropylamine, piperidine, morpholine, pipirazine, N-methyl pipirazine and pyrrolidine. This C-H activation reaction proceeded smoothly to produce the desired products 3a-i in good yields (30-94%). Some of this derivatives with steric hinderance give corresponding secondary amine in low yields (pyrrolidine and diisopropylamine).

The stability and reactivity of 2 mol% Cu^{+2}@GO-PABA nanocatalyst were investigated during the four consecutive runs in model reaction. The stability of copper nanocatalyst displayed any remarkable leaching of the metal in the reactions medium, also a slight activity decrease was detected (Figure 7).
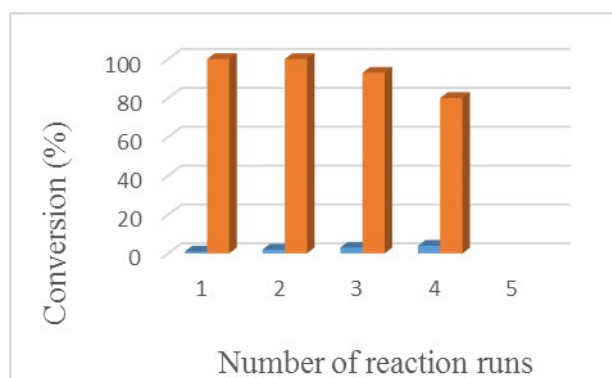
Figure 7. Catalyst reactivity performance

The plausible mechanism has been suggested in Scheme 4, which is accordance with the reaction of tertiary amine reported by Huang.[41] this pathway has three steps. First, the copper species [GO/PABA@Cu^{n+1}] that is oxidized by oxygen, coordinates with the secondary amines to form the intermediate A that is hydrolyzed via CH_3COOH. Then intermediate A coordinates to azole to product B, followed by the subsequent deprotonation/ rearrangment to afford C and recovered CH_3COOH. Finally, the reductive elimination process of C forms the desired product and regenerates the copper catalyst to complete the catalytic cycle of Cu@GO-PABA.
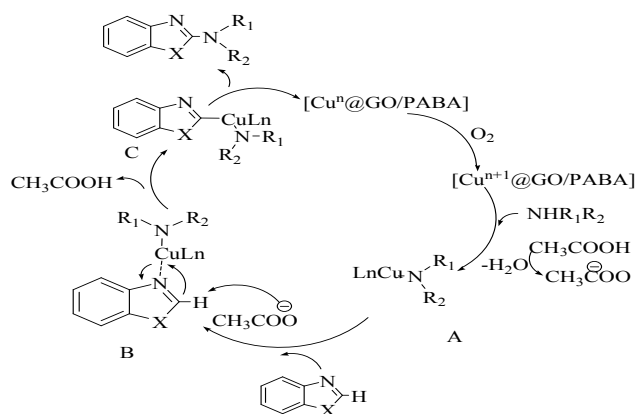
Scheme 4. Proposed mechanism for copper-catalyzed direct oxidative C-H/C-N reaction of azoles.
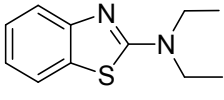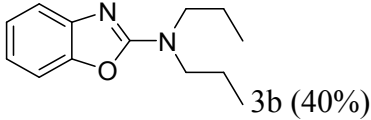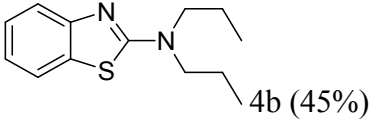
4. CONCLUSION

In Summary, a green, effective and environmentally friendly procedure was reported for the development of heterogeneous Cu (II)-graphene oxide system to carrying out the oxidative sp^2 C-H coupling of benzoxazole and benzothiazole with secondary dialkyle amines under mild condition in O_2 as oxident. Interestingly, the morphology, distribution, and loading of Cu ions could be well-controlled through grafting the graphene oxide with para-amino benzoic acid, and the enhanced catalytic performa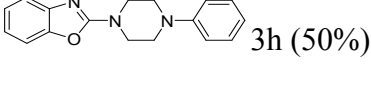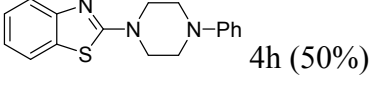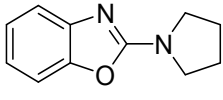nce was achieved for C-H/C-N bond activation reaction. N-Heteroatoms in the para-aminobenzoic acid can accelerate the immobilization of Cu (II) on the graphene oxide surface. Accordingly, the high activity of Cu^{+2}@GO-PABA can be ascribed to the good synergistic effects of Cu^{+2} and para-amino benzoic acid grafted on graphene oxide. Also, Easy work-up, high yield, short reaction time and single-step nature of the methodology are among the main advantages of this procedure.

Conflicts of interest

There are no conflicts to declare.

ARTICLE

Table 2. Copper-Catalyzed Direct C-H Amination of azole
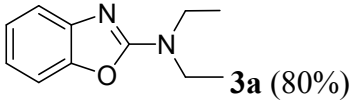
Entry	Product (yield)	
1	**3a** (80%)	4a (94%)
2	3b (40%)	4b (45%)
3	3c (30%)	4c (30%)
4	3d (84%)	4d (94%)
5	3e (53%)	4e (90%)
6	3f (75%)	4f (80%)
7	3g (70%)	4g (70%)
8	3h (50%)	4h (50%)
9	3i (32%)	4i (40%)
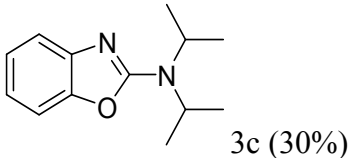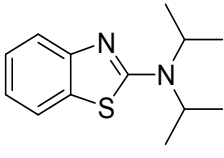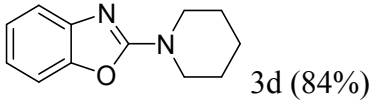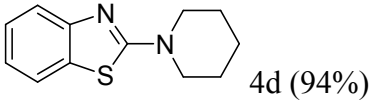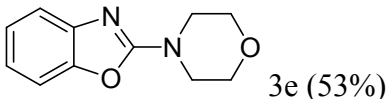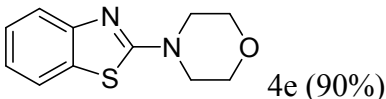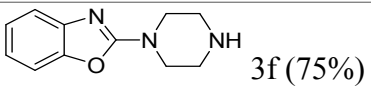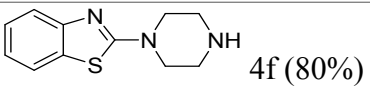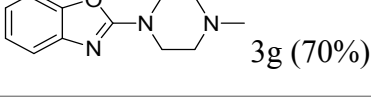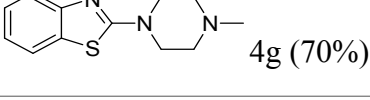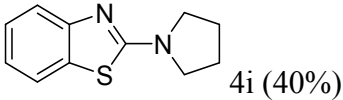
Reaction conditions: azoles (0.5 mmol), amides (2 mL), Cu@PABA-GO (2 mol %), CH$_3$CO$_2$H (120 μL), O$_2$ atmosphere, 70˚C, 12 h.[34] Purification was carried out in chloroform as a solvent.

References

1   R. Hili, A. K. Yudin, *Nat. Chem. Biol*. 2006, **2**, 284; I. V.Seregin, V. Gevorgan, *Chem. Soc. Rev*., 2007, **36**, 1173.
2   Armstrong, A.; Collins, J. C. Direct azole amination: C-H functionalization as a new approach to biologically important heterocycles. Angew. Chem., Int. Ed., 2010, **49**, 2282.

3   A. R. Muci, S. L. Buchwald, *Top. Curr. Chem*. 2002, **219**, 131; D. S. Surry, S. L. Buchwald, *Angew. Chem., Int. Ed*., 2008, **47**, 6338; J. F. Hartwig, *Acc. Chem. Res*., 2008, **41**, 1534.
4   B. Li, H. Cao, J. Shao, G. Li, M. Qu, G. Yin, Co$_3$O$_4$@graphene composites as anode materials for high-performance lithium ion batteries. Inorg. Chem., 2011, **50**, 1628.
5   N. Shang, C. Feng, H. Zhang, S. Gao, R. Tang, C. Wang, Z. Wang, Suzuki–Miyaura reaction catalyzed by graphene oxide supported palladium nanoparticles. *Catal. Commun*., 2013, **40**, 111.

Journal Name

ARTICLE

6 J. Yan, Z. Wang, H. Wang, Q. Jiang, Rapid and energy-efficient synthesis of a graphene–CuCo hybrid as a high performance catalyst. *J. Mater. Chem.*, 2012, **22**, 10990.

7 Q. Chen, L. Zhang, G. Chen, Facile preparation of graphene–copper nanoparticle composite by in situ chemical reduction for electrochemical sensing of carbohydrates. *Anal. Chem.*, 2012, **84**, 171.

8 Y. Zhang, J. Tian, H. Li, L. Wang, X. Qin, A. Asiri, A. Al-Youbi, X. Sun, Biomolecule-assisted, environmentally friendly, one-pot synthesis of CuS/reduced graphene oxide nanocomposites with enhanced photocatalytic performance. *Langmuir,* 2012, **28**, 12893; H. Bahrami, A. Ramazani S. A., A. Kheradmand, M. Shafiee, H. Baniasadi, Investigation of thermomechanical properties of UHMWPE/graphene oxide nanocomposites prepared by in situ Ziegler-Natta polymerization. *Advances in Polymer Technology.*34 (4)

9 W. Chen, L. Yan, P. Bangal, Chemical reduction of graphene oxide to graphene by sulfur-containing compounds. *J. Phys. Chem. C,* 2010, **114**, 19885.

10 B. Garg, Y. Ling, Versatilities of graphene-based catalysts inorganic transformations. *Green Mater*. 2013, **1**, 47.

11 E. Bekyarova, M. Itkis, P. Ramesh, C. Berger, M. Sprinkle, W. Heer, R. Haddon, Chemical modification of epitaxial graphene: Spontaneous grafting of aryl groups. *J. Am. Chem. Soc.*, 2009, **131**, 1336.

12 Berger, C.; Song, Z.; Li, T.; Li, X.; Ogbazghi, A. Y.; Feng, R.; Dai, Z.; Marchenkov, A. N.; Conrad, E. H.; First, P. N.; de Heer, W. A. Ultrathin Epitaxial Graphite: 2D Electron Gas Properties and a Route toward Graphene-Based Nanoelectronics. *J. Phys. Chem. B,* 2004, **108 (52)**, 19912.

13 S. Bae, H. Kim, Y. Lee, X. Xu, J. S. Park, Y. Zheng, J. Balakrishnan, T. Lei, H. Ri Kim, Y. I. Song, Y. J. Kim, K. S. Kim, B. Ozyilmaz, J. H. Ahn, B. H. Hong, S. Iijima, Roll-to-Roll Production of 30-inch Graphene Films for Transparent Electrodes. *Nat. Nano.,* 2010, **5 (8)**, 574.

14 S. Stankovich, D. A. Dikin, G. H. B. Dommett, K. M. Kohlhaas, E. J. Zimney, E. A. Stach, R. D. Piner, S. T. Nguyen, R. S. Ruoff, Graphene-Based Composite Materials. *Nature.* 2006, **442 (7100)**, 282; K. K. Sadasivuni, D. Ponnamma, J., Kim S. Thomas, Graphene-Based Polymer Nanocomposites in Electronics.https://link.springer.com/book/10.1007%2F978-3-319-13875-6.

15 J. J. Yoo, K. Balakrishnan, J. Huang, V. Meunier, B. G. Sumpter, A. Srivastava, M. Conway, A. L. Mohana Yu, J. Reddy, R. Vajtai, P. M. Ajayan, Ultrathin Planar Graphene Supercapacitors. *Nano Lett.*, 2011, **11 (4)**, 1423.

16 W. Yuan, A. Liu, L. Huang, C. Li, G. Shi, High-Performance NO_2 sensors based on chemically modified graphene. *Adv. Mater.*, 2013, **25 (5)**, 766.

17 G. K. Dimitrakakis, E. Tylianakis, G. E. Froudakis, Pillared Graphene: A New 3-D Network Nanostructure for Enhanced Hydrogen Storage. *Nano Lett.*, 2008, **8 (10)**, 3166.

18 K. S. Novoselov, A. K. Geim, S. V. Morozov, D. Jiang, Y. Zhang, S. V. Dubonos, I. V. Grigorieva, A. A. Firsov, Electric Field Effect in Atomically Thin Carbon Films. *Science,* 2004, **306 (5696)**, 666.

19 A. K. Geim, K. S. Novoselov, The rise of Graphene. *Nat. Mater.*, 2007, **6 (3)**, 183.

20 C. Lee, X. Wei, J. W. Kysar, J. Hone, Measurement of the Elastic Properties and Intrinsic Strength of Monolayer Graphene. *Science,* 2008, **321 (5887)**, 385.

21 A. A. Balandin, S. Ghosh, W. Bao, I. Calizo, D. Teweldebrhan, F. Miao, C. N. Lau, Superior Thermal Conductivity of Single-Layer Graphene. *Nano Lett.*, 2008, **8 (3)**, 902.

22 A. N. Obraztsov, E. A. Obraztsova, A. V. Tyurnina, A. A. Zolotukhin, *Carbon,* 2007, **45**, 2017.

23 Li, X.; Cai, W.; An, J.; Kim, S.; Nah, J.; Yang, D.; X. Li, W. Cai, J. An, S. Kim, J. Nah, D. Yang, R. Piner, A. Velamakanni, I. Jung, E. Tutuc, S. K. Banerjee, L. Colombo, R. S. Ruoff, *Science,* 2009, **324**, 1312.

24 A. Reina, X. Jia, J. Ho, D. Nezich, H. Son, V. Bulovic, M. S. Dresselhaus, Kong, *J. Nano Lett.*, 2009, **9**, 30.

25 J. Coraux, A. T. N'Diaye, C. Busse, T. Michely, *Nano Lett.*, 2008, **8**, 565.

26 L. Gao, J. R. Guest, N. P. Guisinger, *Nano Lett.*, 2010, **10**, 3512; Sharmila, T. K. Bindu, S. Sreesha, N. R. Suja, P. M. S. Beegum, E. T. Thachil, A comparative investigation of aminosilane/ethylene diamine–functionalized graphene epoxy nanocomposites with commercial and chemically reduced graphene: static and dynamic mechanical properties. *Emergent Materials.* 2019, **2 (3)**, 371-386; P. Nagaraju, R. Vasudevan, M. Arivanandhan, A. Alsalme, R. Jayavel, High-performance electrochemical capacitor based on cuprous oxide/graphene nanocomposite electrode material synthesized by microwave irradiation method. *Emergent Materials*, 2019, 2**(4)**, 495-504; W. Zhiqing, N. Ambrožová, E. Eftekhari, N. Aravindakshan, W. Wang, Q. Wang, S. Zhang, K. Kočí, Q. Li, Photocatalytic H_2 generation from aqueous ammonia solution using TiO_2 nanowires-intercalated reduced graphene oxide composite membrane under low power UV light. *Emergent Materials*, 2019, **2 (3)**, 303-311.

27 W. Hummers, R. Offeman, Preparation of graphitic oxide. *J. Am. Chem. Soc.*, 1958, **80**, 1339.

28 Y. Si, E. Samulski, Synthesis of water soluble graphene. *Nano Lett.*, 2008, **8**, 1679.

29 H. He, C. Gao, General approach to individually dispersed highly soluble and conductive graphene nanosheets functionalized by nitrene chemistry. *Chem. Mater.*, 2010, **22**, 5054.

30 V. Georgakilas, A. Bourlinos, R. Zboril, T. Steriotis, P. Dallas, A. Stubos, C. Trapalis, Organic functionalisation of graphenes. *Chem. Commun. (Cambridge, U. K.)* 2010, **46**, 1766.

31 B. Kerscher, A. Appel, R. Thomann, R. Mülhaupt, Treelike polymeric ionic liquids grafted onto graphene nanosheets. *Macromolecules,* 2013, **46**, 4395.

32 S. Deng, V. Tjoa, H. Fan, H. Tan, D. Sayle, M. Olivo, S. Mhaisalkar, J. Wei, C. Sow, Reduced graphene oxide conjugated Cu_2O nanowire mesocrystals for high-performance NO2 gas sensor. *J. Am. Chem. Soc.*, 2012, **134**, 4905.

33 D. C. Marcano, D. V. Kosynkin, J. M. Berlin, A. Sinitskii, Z. Sun, A. Slesarev, *ACS Nano.*, 2010; **4**: 4806; R. S. Dey, S. Hajra, R. K. Sahu, C. R. Raj, M. K. Panigrahi, *Chemical Communications,* 2012; **48**, 1787.

34 L. Yaming, X. Yusheng, Z. Rong, J. Kun, W. Xiuna, D. Chunying, *J. Org. Chem.*, 2011, **76**, 5444.

35 Y. −T. Liu, M. Dang, X. -M. Xie, Z. -F. Wang, X.-Y. Ye, Synergistic effect of Cu^{2+}-coordinated carbon nanotube/graphene network on the electrical and mechanical properties of polymer nanocomposites. *J. Mater. Chem.*, 2011, **21**, 18723.

36 Y. Matsumoto, M. Koinuma, S. Ida, S. Hayami, T. Taniguchi, K. Hatakeyama, H. Tateishi, Y. Watanabe, S. Amano, Photoreaction of Graphene Oxide Nanosheets in Water. *J. Phys. Chem. C,* 2011, **115**, 19280; Y. Matsumoto, M. Morita, S. Y. Kim, Y. Watanabe, M. Koinuma, S. Ida, Photoreduction of Graphene Oxide Nanosheet by UV-light illumination under H_2. *Chem. Lett.,* 2010, **39**, 750; Y. Matsumoto, M. Koinuma, S. Y. Kim, Y. Watanabe, T. Taniguchi, K. Hatakeyama, H. Tateishi, S. Ida, Simple Photoreduction of Graphene Oxide Nanosheet Under Mild Conditions. *ACS Appl. Mater. Interfaces,* 2010**, 2**, 3461; F. Zhao, J. Liu, X. Huang, X. Zou, G. Lu, P. Sun, S. Wu, W. Ai, M. Yi, X. Qi, L. Xie, J. Wang, H. Zhang, W. Huang, Chemoselective Photodeoxidization of Graphene Oxide Using Sterically Hindered Amines as Catalyst: Synthesis and Applications. *ACS Nano,* 2012, **6**, 3027.

37 Zhu, C.; Guo, S.; Fang, Y.; Dong, S. Reducing Sugar: New Functional Molecules for the Green Synthesis of Graphene Nanosheets. ACS Nano 2010, 4, 2429–2437.

38 J. Zhu, G. Zeng, F. Nie, X. Xu, S. Chen, Q. Han, X. Wang, Decorating Graphene Oxide with CuO Nanoparticles in a Water-Isopropanol System. *Nanoscale,* 2010, **2 (6)**, 988.

39 C. Xu, X. Wang, J. Zhu, X. Yang, L. Lu, Deposition of Co_3O_4 Nanoparticles onto Exfoliated Graphite Oxide Sheets. *J. Mater. Chem*., *2008*, **18 (46)**, 5625.

40 P. Fakhri, B. Jaleh, M. Nasrollahzadeh, Synthesis and characterization of copper nanoparticles supported on reduced graphene oxide as a highly active and recyclable catalyst for the synthesis of formamides and primary amines. *J. Mol. Catal. A: Chem*., 2014, **383–384**, 17.

41 S. Guo, B. Qian, Y. Xie, C. Xia, H. Huang, Copper-catalyzed oxidative amination of benzoxazoles via C–H and C–N bond activation: a new strategy for using tertiary amines as nitrogen group sources. Org. Lett., 2011, **13 (3)**, 522.
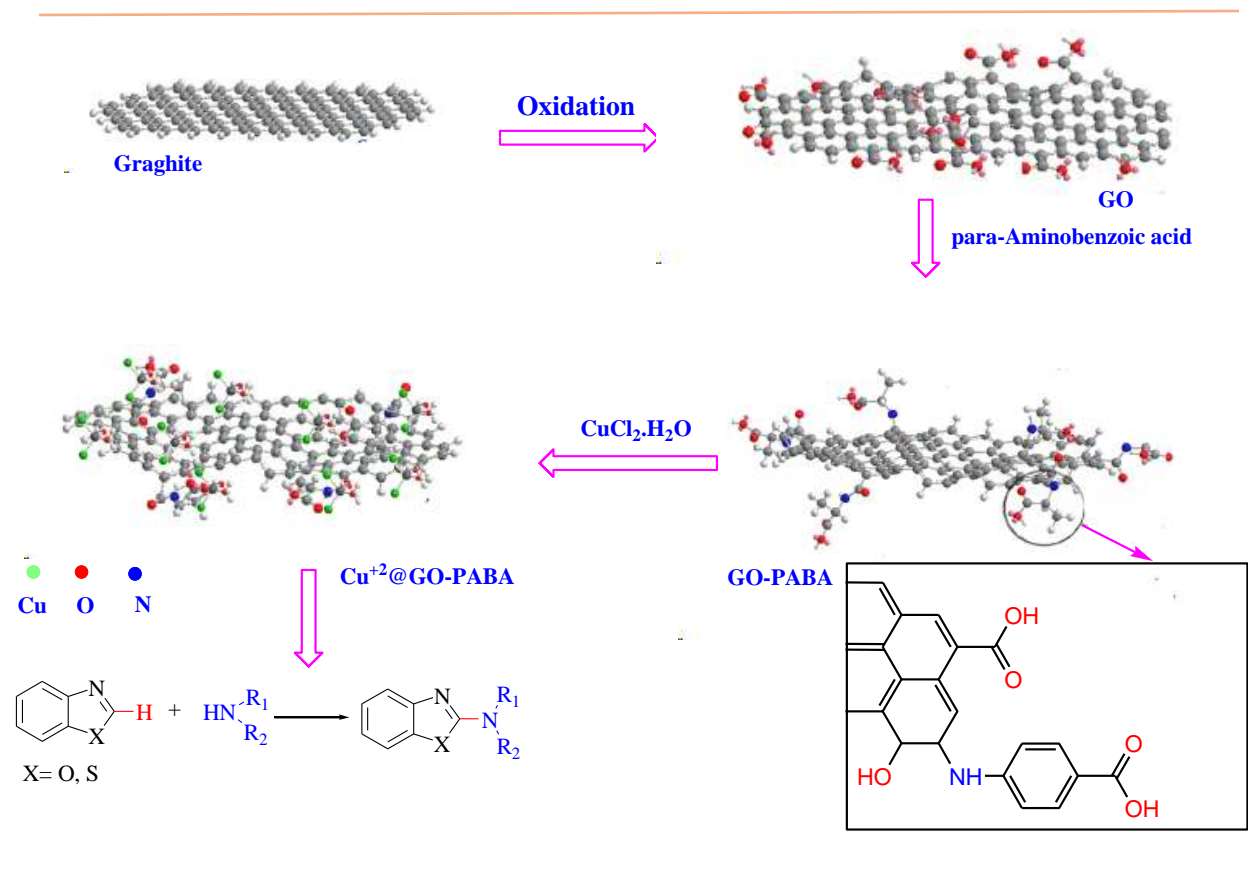
New Journal of Chemistry Accepted Manuscript

Graphical Abstract

Copper (II) ions Supported on Functionalized Graphene Oxide: An Organometallic Nanocatalyst for Oxidative Amination of Azoles via C–H/ C-N Bond Activation azoles

Masoumeh Behzadi,*[a] Mohammad Mahmoodi Hashemi,*[a] Mostafa Roknizadeh,[a] Shahrokh Nasiri,[a] Ahmad Ramazani Saadatabadi[b]

[a]Department of Chemistry, Sharif University of Technology,Tehran, Iran.
[b]Department of Chemical and Petroleum Engineering, Sharif University of Technology, Tehran, Iran.